# OpenStreetMap for Multi-Faceted Climate Risk Assessments

**Evelyn Mühlhofer**

Institute for Environmental Decisions, ETH Zurich, Zurich, 8092, Switzerland

**Chahan M. Kropf**

Institute for Environmental Decisions, ETH Zurich, Zurich, 8092, Switzerland
Federal Office of Meteorology and Climatology MeteoSwiss, Zurich-Airport, 8058, Switzerland

**Lukas Riedel**

Institute for Environmental Decisions, ETH Zurich, Zurich, 8092, Switzerland
Federal Office of Meteorology and Climatology MeteoSwiss, Zurich-Airport, 8058, Switzerland

**David N. Bresch**

Institute for Environmental Decisions, ETH Zurich, Zurich, 8092, Switzerland
Federal Office of Meteorology and Climatology MeteoSwiss, Zurich-Airport, 8058, Switzerland

**Elco E. Koks**

Institute for Environmental Studies, VU Amsterdam, Amsterdam, the Netherlands

E-mail: `evelyn.muehlhofer@usys.ethz.ch`

4 September 2023

**Abstract.** Natural hazards pose significant risks to human lives, infrastructure, and ecosystems, necessitating a comprehensive understanding of climate risks for effective adaptation planning and risk management. However, climate risk assessments mostly focus on economic asset values and infrastructures such as roads and buildings, because publicly available data on more diverse exposures are scarce. The increasing availability of crowd-sourced geospatial data, notably from OpenStreetMap, opens up a novel means for assessing climate risk to a large range of physical assets. To this end, we present a stand-alone, lightweight, and highly flexible Python-based OpenStreetMap data extraction tool: OSM-flex. We demonstrate the potential and limitations of OpenStreetMap data for risk assessments by coupling OSM-flex to the open-source natural hazard risk assessment platform CLIMADA, and computing the current climate's winter storm risk and event impacts from the severe winter storm Lothar across Switzerland. Specifically, we evaluate the risks and impacts on forests, UNESCO heritage sites, railways, healthcare facilities, and airports, and compare them with traditional impact metrics such as asset damages and affected population. This study aims to provide researchers, practitioners, and decision-makers with insights into utilizing open-source data and software tools for conducting multi-faceted and high-resolution climate risk assessments.

## 1. Introduction

Natural hazards affect humans, human-made structures, and nature. Impacts and consequences of such events may therefore be as diverse as the exposed assets. Understanding these multiple dimensions of disaster risk across economic, social, health, educational, environmental, and cultural heritage is also a main priority within the Sendai Framework for Disaster Risk Reduction (UNDRR 2015, § 24 f). While capturing many facets of risk incurred by natural hazard events can allow for better and more informed risk management practices, capabilities to do so are often severely constrained by data availability within all stages of the risk assessment chain - not least on the exposure side.

The Sendai Framework, therefore, stresses the importance of access to reliable data, including geographic information systems (GIS), to "strengthen technical and scientific capacity to capitalize on and consolidate existing knowledge and to develop and apply methodologies and models to assess disaster risks, vulnerabilities, and exposure to all hazards" (UNDRR 2015). As the research community and decision-makers are urged to move towards more diverse analyses of natural hazard-induced risks in a changing climate, open-source tools are needed to facilitate these in an equitable manner that is accessible to a wider range of stakeholders.

Responding to this need, models to capture risk—defined as the product of hazard, exposure and vulnerability by the IPCC (Field et al. 2014)—are increasingly developed in an open-source manner (e.g., Aznar-Siguan and Bresch 2019; Paulik et al. 2022; Koks 2022). However, many off-the-shelf input data sets for risk computations may not have global coverage, and bespoke models frequently focus

on a single component of the risk equation, especially on the hazard side (cf. Bloemendaal, Haigh, et al. 2020; Yamazaki et al. 2011; Lüthi et al. 2021; Pagani et al. 2022). Moreover, interoperability between models and data sets covering different risk components is often not straightforward, reducing usability for non-experts despite their (theoretical) availability.

Nevertheless, the advancement of remote sensing has greatly aided the development of spatially explicit global exposure layer data, such as building footprints (Microsoft 2023), population counts (Center for International Earth Science Information Network (CIESIN), Columbia University 2017; WorldPop and Center for International Earth Science Information Network (CIESIN), Columbia University 2020), land use and land cover (Potapov et al. 2022) or economic asset value concentrations (Eberenz et al. 2020). While this offers obvious potential for natural hazard risk assessments, the aspects of risk which can be explored with these data sets are inherently constrained to economic values and population numbers.

The increasing level of detail with which the visible environment is mapped in OpenStreetMap (OSM) offers different and less conventional opportunities for natural hazard risk assessment (Nirandjan et al. 2022). As a freely available and open-source resource for geo-referenced exposure data, OSM has been used as an input layer in a number of studies in the wider area of natural hazard risks, spanning direct damage assessments (Koks, Rozenberg, et al. 2019), service disruptions (Mühlhofer, Koks, Kropf, et al. 2023), emergency response (Gultom, Haryanto, and Suhartanto 2021) and adaptation planning (Schotten and Bachmann 2023). Many of them focus predominantly on general building stocks (Cerri et al. 2021; Bloemendaal and Koks 2022) and major transportation assets such as roads and railways

(Koks, Rozenberg, et al. 2019; Mulholland and Feyen 2021; van Ginkel et al. 2021), and to a lesser degree on other (critical) infrastructure assets such as airports (Yesudian and Dawson 2021), social facilities (Nirandjan et al. 2022; Mühlhofer, Koks, Kropf, et al. 2023) or power generation and distribution assets (Nirandjan et al. 2022). However, as it is not limited to modern human-made structures, the OSM data supports the study of other risk areas of the built-up and natural environment, such as forests, agricultural land, UNESCO heritage sites, and ecosystem services (Ruckelshaus et al. 2020).

Although a number of Python tools have been developed for the retrieval of certain high-resolution exposure data from OSM (e.g., Tenkanen 2020; Boeing 2017), there is no versatile linkage to access the entire data universe and efficiently perform natural hazard risk assessments on these data on a large scale.

The aim of this study is thus three-fold: first, to bridge a data access gap by presenting the lightweight, stand-alone, and highly flexible Python module OSM-flex (Mühlhofer, Koks, Riedel, et al. 2023) that enables users to efficiently and consistently retrieve geospatial exposure data from OSM with all available information; second, to demonstrate seamless integration within the open-source natural hazard risk assessment platform CLIMADA (Aznar-Siguan and Bresch 2019) to perform end-to-end risk assessments; and third, to show that more diverse perspectives of natural hazard-induced risks, and hence risk management strategies, may be explored when opening up to the potentials of non-conventional exposure data.

Within a brief case study on winter storm impacts to railroads, hospitals, UNESCO heritage sites, airports, and forests in Switzerland, yet without loss of generality, we illustrate the major implementation steps, assumptions, limitations, and decision-making implications involved in computing event impacts and natural hazard risks from high-resolution exposure data obtained through OSM. By providing these open-source tools and perspectives, we aim to raise awareness and broaden the means for exploring non-monetary facets of climate risk.

## 2. Methods

### 2.1. Obtaining Geospatial Data from OSM with OSM-flex

Features can be extracted from OSM and converted into geographical tabular format for use in Python in two ways: either by reading data directly from the Overpass API‡ or by downloading regional data dumps as Protocolbuffer Binary Format (PBF) files§ from dedicated online repositories such as GeoFabrik (2023), from which the desired data can then be parsed.

Two well-known Python packages, Pyrosm (Tenkanen 2020) and OSMnx (Boeing 2017), excel at opposite ends of this retrieval spectrum. Both packages are well maintained and easily installable using standard package managers. While a core functionality of both packages is the selective parsing of geographical features from OSM into Python-based tabular formats, OSMnx features additional integration with graph-analysis packages and common plotting libraries. Because OSMnx relies on API queries for data retrieval, it is limited by restrictions on query sizes and requires a constant internet connection for this process. Pyrosm circumvents this by parsing

‡ See `https://overpass-api.de/`
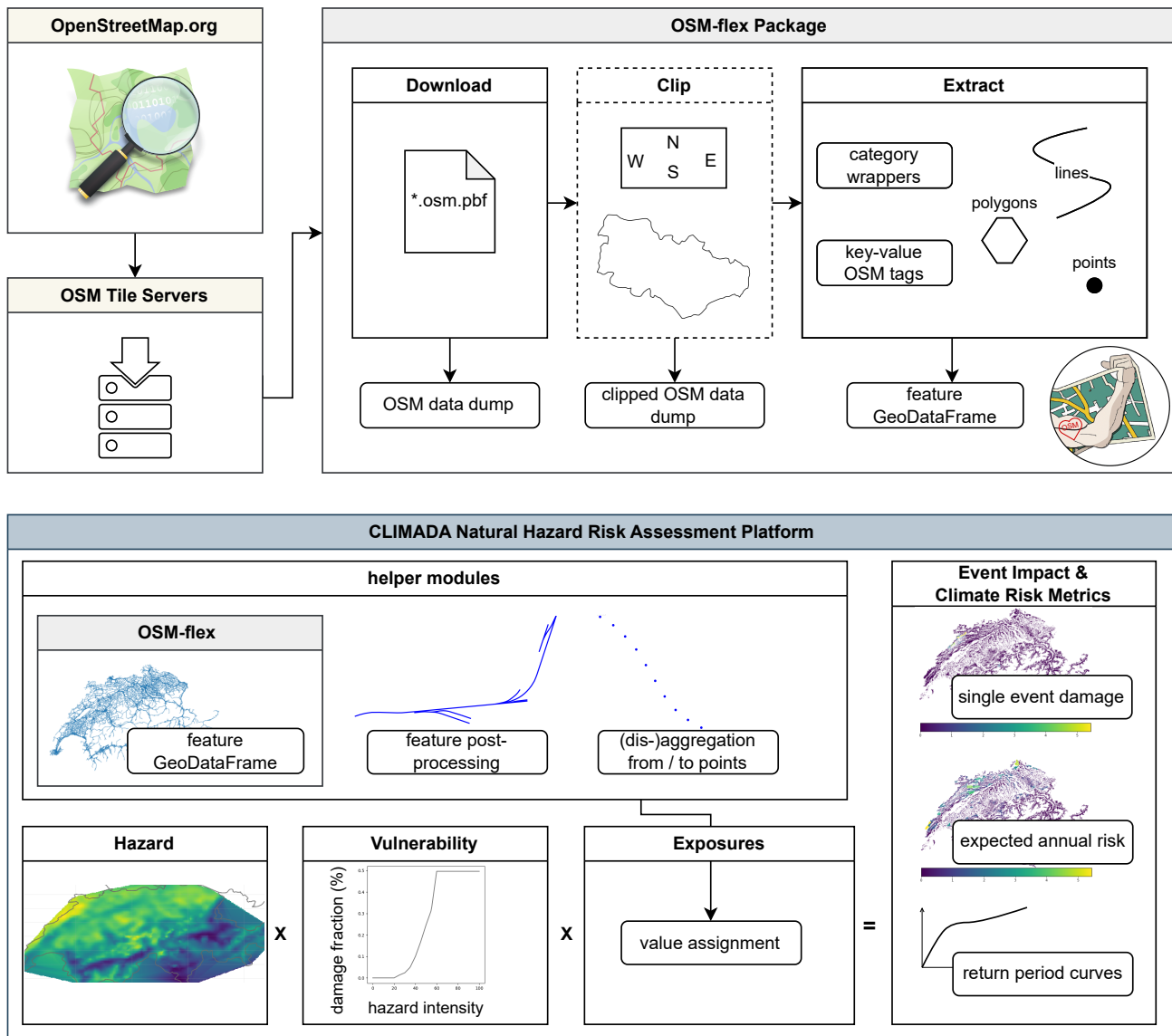§ See `https://wiki.openstreetmap.org/wiki/PBF_Format`

**Figure 1.** Schematic representation of a climate risk assessment workflow for OSM features using the OSM-flex package and CLIMADA. Top panel: basic steps for OSM feature extraction in the OSM-flex module: an OSM data dump is downloaded in *.osm.pbf format; optionally the area is clipped to an arbitrary polygon shape; the elements of interest are extracted using pre-written or custom queries with OSM tags; the data is converted into a GeoDataFrame. Bottom panel: integration of OSM data into the CLIMADA risk assessment workflow. The helper modules within CLIMADA conveniently allow users to directly derive point-based CLIMADA Exposures by accessing the OSM-flexmodule and dissaggregating lines and polygons exposure elements to points. The obtained point exposure can then be combined with the hazard and vulnerability models to compute point impacts (risk). Finally, point-based impact and risk data can be re-aggregated to the original OSM feature geometries.

downloaded data dumps, yet relies on OSMnx in the background for other functionalities. Both come with a range of non-standard package dependencies and vary in customizability of the queries in terms of spatial areas and specification of filtering attributes.

Here, we introduce the lightweight Python-based package OSM-flex (Mühlhofer, Koks, Riedel, et al. 2023), which efficiently parses large sets of OSM data based on user-specified queries from PBF data dumps within arbitrary and fully user-defined geographical boundaries, such as cities, states, multi-country regions or bounding boxes. This provides the computational efficiency and user flexibility required to perform multi-faceted risk analyses. Its availability on common software distribution channels (PyPI and GitHub) and its low dependency requirements make it suitable for integration within larger and more complex software packages such as the CLIMADA risk assessment platform discussed in section 2.2. The package repository features a test suite that is executed in an automated testing pipeline. Appendix B provides an in-depth comparison of all three above-mentioned packages to guide interested researchers in the selection process for the most-suited tool given their research ambitions.

The general workflow of the OSM-flex package includes four steps, as illustrated in the upper panel of Fig. 1:

(i) **Download** a country, regional or planet data dump (PBF file) from an online repository

(ii) **Clip** the data dump to the area of interest (optional)

(iii) **Extract** the desired features from OSM into tabular format using the OSM tagging syntax

(iv) **Post-process** the extracted data set (optional)

OSM-flex favors the one-time download of PBF data dumps over the direct query of individual features from the Overpass API, as feature extraction does not require a constant internet connection nor is constrained by query size limitations. Appendix A.1 provides details on what access points and (regional) versions of data dumps are readily obtainable within OSM-flex.

The optional step of clipping a larger data dump to specific bounding boxes or (multi-)polygons is useful when dealing with regions or small islands that are not available as dedicated files on one of the OSM data repositories, or when wanting to clip from, for example, the global level along own predefined borders. It currently requires manual installation of the small command-line executable `osmconvert`‖ which facilitates the clipping commands within OSM-flex. In future iterations of OSM-flex, this step may be further simplified. See Appendix A.2 for details on clipping options and these tools.

While OSM-flex is built to be lean and accessible, its use requires some familiarization with the syntax of keys and values in OSM, that is, the attributes that characterize geolocated data and allow it to be queried. For increased user friendliness, common exposure data categories can also be retrieved with pre-written extraction wrappers, such as road and railway assets, healthcare and education facilities, or power infrastructure. Additional details are provided in Appendix A.3.

The desired geospatial information with point-, line-, and polygon-based object geometries and attribute columns is provided as a

‖ See `https://wiki.openstreetmap.org/wiki/Osmconvert`

GeoDataFrame, a data type defined by the GeoPandas Python package (Bossche et al. 2023). After obtaining the data, further post-processing may be required, such as filtering out very small, yet numerous polygons belonging to large natural areas, removing duplicates, or simplifying transportation network geometries. See Appendix A.4 for helpful post-processing resources and steps.

More extensive code documentation and detailed tutorials featuring usage examples are available at `https://osm-flex.readthedocs.io` to guide users. Starting from the possibility of extracting a wide range of exposure data from OSM, the following paragraph outlines how this data can be efficiently integrated into a climate risk assessment workflow.

## 2.2. Using OSM Features in Climate Risk Assessments with CLIMADA

CLIMADA is an open-source Python platform for natural hazard impact computations, climate risk assessments, and adaptation option appraisal (Aznar-Siguan and Bresch 2019; Bresch and Aznar-Siguan 2021). It computes risk according to the IPCC risk definition as the product of exposure, vulnerability, and hazard (Pörtner et al. 2022). Hazard represents events as spatially explicit footprints with an associated hazard-specific intensity metric such as flood depth or wind speed. Each event can be assigned an occurrence probability to form a probabilistic set. Exposures are a spatially explicit representation of the elements potentially at risk, including their (non-)monetary value such as population clusters with population counts or infrastructure assets with their production capacity. Vulnerability is the linking element between hazard and exposure, and is modeled as an impact function relating the hazard intensity to the expected impact, expressed in a ratio of exposure value.

Exposure data which represents the spatial distribution of monetary asset values (Eberenz et al. 2020) or population counts most commonly forms the basis of climate risk assessments. CLIMADA is flexible with regard to input data, thus allowing arbitrary exposure inputs, vulnerability function definitions, and hazard footprints.

To perform such a risk analysis on OSM features, exposure data must first be extracted into a GeoDataFrame as described in Section 2.1. As CLIMADA's engine is designed only for pointwise data, line- and polygon-based data must be interpolated to points before the impact computations, and re-aggregated afterwards, which can be done with a dedicated utility module (see Appendix C for the logic of this helper module and (dis-)aggregation options). Similarly, dedicated hazard and vulnerability data must be provided and can be obtained via the CLIMADA data API for several hazards (Schmid 2023) or be ingested from users' own resources.

## 3. Application: A Multi-Faceted View on Winter Storm Risk

On December 26, 1999, winter storm *Lothar* swept across France, Germany and Switzerland, leaving a trace of destruction. In Switzerland, the event is among the top three most impactful winter storms, with significant tolls on human lives, critical infrastructure, building damage, forest loss, and wildlife (Gaillard et al. 2003; Jordi 2019; Niemeyer and Albisser 2001).

In the following sections, the methodology presented above is explored by computing the wind impacts of Lothar on OSM-extracted built-up and natural assets across Switzerland.

The results are compared with more conventional metrics such as the total value of physical assets damaged and the number of people affected, and validated with event reports. Furthermore, the average annual risk of winter storms to these exposures, obtained from a probabilistic hazard set representing today's climate, is reported.

### 3.1. Winter Storm Impact Calculations with OSM and CLIMADA

*3.1.1. OSM Exposure Data Extraction* Using OSM-flex, OSM data from Switzerland was downloaded from `https://geofabrik.de` on March 13, 2023. Points, lines and polygon data were extracted into GeoPandas GeoDataFrames for 1155 major healthcare facilities (hospitals, clinics, and doctors' practices), 20 100 km of railways (individual rails, incl. trams and narrow gauge rails), 15 airports, 12 500 km$^2$ of forests, and 11 UNESCO heritage sites, see Fig. D2. The exact queries (OSM tags) are noted in Table D1. Geospatial data were post-processed to eliminate very small areas ($< 100$m$^2$) of forest, and duplicates for healthcare facilities and airports.

*3.1.2. Wind Impact* The wind field of storm Lothar was prepared by Welker, Röösli, and Bresch (2020) as the maximum 3-second sustained wind speeds at a height of 10 m above ground over 72 h at a spatial resolution of approximately 4.4 km, based on the Windstorm Information Service (WISC) of the Copernicus Climate Change Service. These data were obtained via the CLIMADA Data API and stored as a CLIMADA Hazard object, see Fig. D1. OSM data were stored as CLIMADA Exposure objects, together with a general asset value exposure for Switzerland based on the product of nightlight intensity and population count data at 30 arcsecond resolution (LitPop, (Eberenz et al. 2020)), and a population exposure at the same resolution based on the SEDAC GPW v4.0 dataset (Center for International Earth Science Information Network (CIESIN), Columbia University 2017); see Fig. D3). Impact functions (vulnerability curves) relating hazard intensity to damage extent were obtained from (Welker, Röösli, and Bresch 2020) for wind-induced general asset damages, which were calibrated to the Swiss context. For all other exposures, step functions were employed that mirror warning categories issued by the Swiss Federal Office of Meteorology and Climatology (MeteoSwiss 2023; Blass et al. 2022). For population, railways, healthcare facilities and airports, wind intensities above 30.5 m/s (110 km/h, warning category 4) were considered critical based on the warning rationales provided by official sources, whereas for forests, wind intensities above 38.9 m/s (140 km/h, warning category 5) were considered more adequate to capture tree snapping (Virot et al. 2016). See Fig. D4 for the plots of all impact functions used. Impacts were computed for all exposures within the CLIMADA, whereby line and polygon-based data (i.e. railways and forests) were interpolated to a 100 m resolution and re-aggregated (by summation) afterwards into their original shapes. The impact data are shown in Fig. 2.

*3.1.3. Wind Risk* In addition to the extreme storm Lothar, we also considered the general winter storm risk in Switzerland following the IPCC definition of risk as the probability of occurrence of an event multiplied by its severity. To this effect, we used the WISC probabilistic extension hazard event set, available through the CLIMADA Data API (Röösli and Bresch 2020; Welker, Röösli, and Bresch 2020). This hazard set is

**Table 1.** Impacts from winter storm Lothar (1999) across Switzerland for general asset values, population counts, and five categories of OSM-retrieved exposures.

| Exposure type | Absolute | Relative |
|---|---|---|
| Asset Values[a] | US \$179.4 mil. | 0.01% |
| Population[a] | 4.17 mil. people | 57.2% |
| Healthcare Facilities[b] | 649 units | 56.2% |
| Airports | 6 units | 40.0% |
| UNESCO Sites | 3 sites | 27.3 % |
| Railways[c] | 6 951 km | 50.4% |
| Forests | 464.6 km² | 3.7% |

[a] reference year: 2000; [b] hospitals, clinics and doctors' offices; [c] all individual lines counted separately, also for parallel tracks.

based on historic records, but features an additional 29 synthetic hazards per historic hazard occurrence from 1940 to 2014. It was calibrated on the years 1990–2010, which can be seen as representative of climate conditions today. Furthermore, for the physical asset and population exposure layers, we used the reference year 2020 instead of 1999.

*3.2. Results*

Table 1 summarizes the impacts of storm Lothar computed for different exposures. Although affected by varying absolute and relative degrees, the impacts are considerable across all studied dimensions. An important distinction must be made with regards to what these impact figures stand for: For forests and general asset values, physical losses and damages are modelled; for the remaining exposure categories, the numbers of items *exposed* to a certain hazard intensity are modelled without direct implications of the extent of loss or damage, as no such impact functions were available in the concrete case.

Comparison with print media accounts, official records, insurance reports, and the compilation by Niemeyer and Albisser (2001) confirms the severity of the event across many dimensions of (public) life and strengthens the picture of multi-faceted impacts obtained from the computations presented in this study: reported impact metrics tend to revolve around (insured) building damages (in the case of Lothar, around CHF 600 mil.) and affected population or fatalities (15 people died during the storm, and roughly the same amount afterwards during clean-up and reconstruction efforts). The standard impact computations within CLIMADA capture these metrics as asset damages (though under-estimated with US \$179 mil. or CHF 113.3 mil. at the time), and affected population (4.17 mil., a number that is inherently difficult to track and verify, as reports tend to focus on the well-reported number of fatalities instead). However, other dimensions of societal importance were equally captured, such as rail transportation - mapped here as affected to roughly 50 % - was indeed interrupted on many lines across the German-speaking part of Switzerland (covering approximately 65 % of Swiss territory); estimated forest losses (amounting to CHF 750 mil. in economic worth, and 4.3% of the Swiss forest area), is close to the modelled 3.7% of the area. It was not possible to retrieve explicit reports on the impacts to airports (apart from flight cancellations), healthcare facilities or UNESCO heritage sites. Not modelled within the scope of this illustrative case-study, but frequently mentioned in reports were impacts on the power grid and road transportation (Niemeyer and Albisser 2001). While structural impacts on the latter may be easily computed with the presented approach, modelling systemic impacts on the energy sector is not only restrained by power line mapping quality on OSM, but would also require consideration of the cascades of failing infrastruc-

**Table 2.** Average annual risk from winter storms across Switzerland for general asset values, population counts and five categories of OSM-retrieved exposures.

| Exposure type | Absolute | Relative |
|---|---|---|
| Asset Values[a] | US $4.8 mil. | 0.0003% |
| Population[a] | 91'200 people | 1.3% |
| Healthcare Facilities[b] | 14.4 units | 1.3% |
| Airports | 0.5 units | 1.2% |
| UNESCO Sites | 0.08 sites | 0.7% |
| Railways[c] | 17.3 km | 1.3% |
| Forests | 9.83 km$^2$ | 0.08% |

[a] reference year: 2020; [b] hospitals, clinics and doctors' practices; [c] all individual lines counted separately, also for parallel tracks

tures (Mühlhofer, Koks, Kropf, et al. 2023). The results highlight that, when using multiple exposure layers, important aspects of a natural hazard event beyond conventionally reported (undifferentiated) asset damages can be captured relatively effortlessly, and guide risk management efforts.

As introduced in Section 3.1.3, it may be insightful to consider probabilistic risk metrics apart from single-hazard event impacts, to gauge the potential risk landscape and to adequately place the occurrence of historic events therein. Various metrics may be relevant, such as the risk associated with a one-in-a-hundred-year event or the average annual risk. Table 2 presents the latter, modelled from the probabilistic winter storm set. Evidently, since most winter storms are less extreme than Lothar (cf. Table 1), the average annual risk values are much lower (less than 1.5% of the total count or value for all exposure categories). The extremes of Lothar's impacts are even more strikingly illustrated when locating these impact figures on return period curves generated from the probabilistic hazard set (Fig. D5). With return periods between roughly 80 and 150

years depending on the choice of exposure category, this highlights the potential for disastrous consequences of tail risk events as compared to the average, in particular for non-monetary elements. Furthermore, as shown in Fig. D6, the average annual expected impacts are inhomogeneously distributed, with distinct patterns for the different exposure types. For instance, regular impact on forestry is mostly expected in Western Switzerland in the Jura mountain chain, whereas asset damages are concentrated in the regions around Basel and Zurich, and certain train lines in central Switzerland and alpine valleys may be often affected.

Studies have also demonstrated that, under a rapidly changing climate, winter storm risk, as measured in losses to general asset values, may increase by up to 50% between 2020 and 2050, both for average events and for more extreme events (Severino et al. 2023). This increase might bring significant economic challenges, yet does not provide a full picture of the potential for disruption of the railway system, or the losses to vital forest ecosystems and irreplaceable cultural sites, which may hence be explored using the demonstrated workflow.

## 4. Discussion

We showed how OSM-flex, a flexible OSM feature extraction package, can be seamlessly integrated into the CLIMADA risk modelling framework, and how this can provide a basis for multi-faceted natural hazard impact and climate risk assessments on a variety of exposure types. The case study, though brief and mainly illustrative of the major steps and processes of using OSM for climate risk assessments, demonstrated that the readily computed event impacts from winter storm Lothar
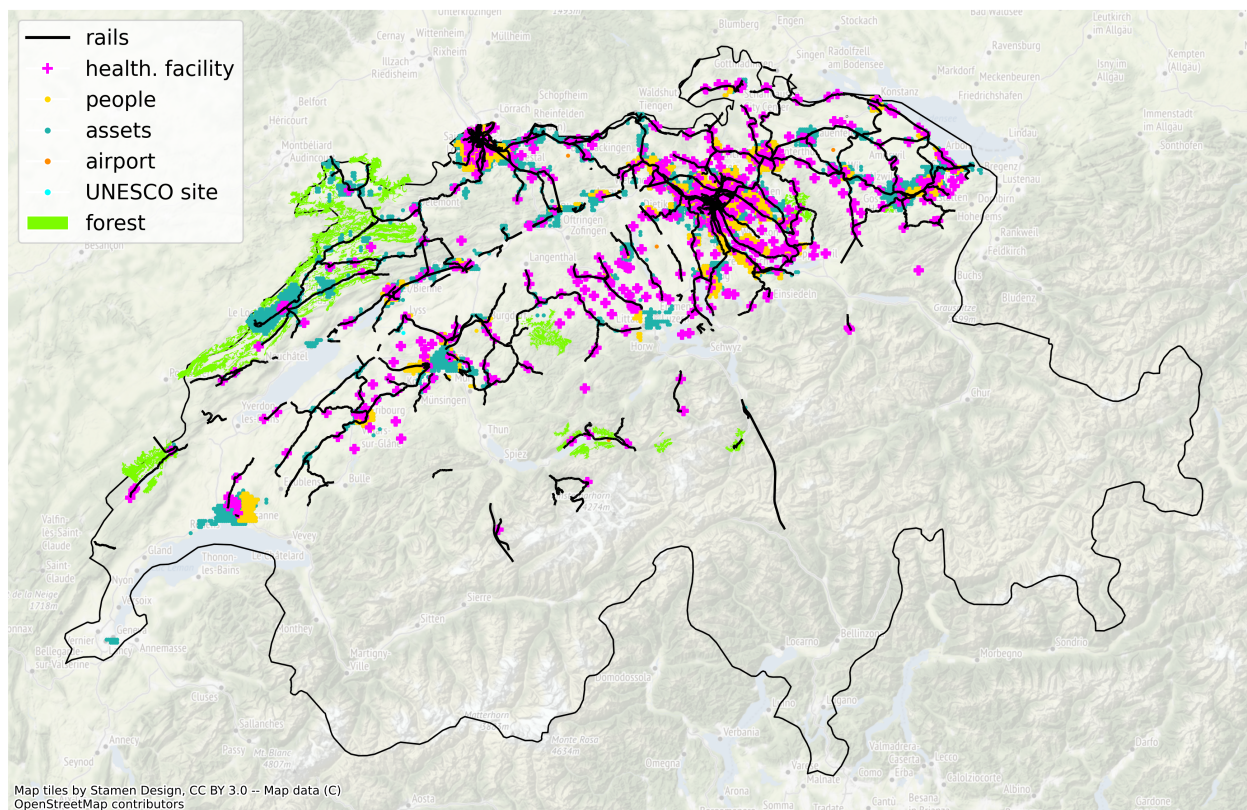
**Figure 2.** Geographical representation of all impacted elements by storm Lothar (c.f. Table 1). For visual clarity, only asset value grid cells and population grid cells with impacts above 10 000 $ and 1 000 persons, respectively, are shown. Note that in certain areas (e.g. around the city of Zurich in the North-East) many impacts overlap.

on rails and on forests in Switzerland came remarkably close to the actual event estimates, which were collected in meticulous survey work at the time (Niemeyer and Albisser 2001), hence providing an efficient way to quickly estimate damages also to sectors which are not closely and easily monitored. Probabilistic estimates for winter storm risks further revealed that risk hot-spots differ spatially for different exposure categories, which may hence guide more targeted adaptation planning. Moreover, contrasting impacts derived from less conventional exposure layers such as UNESCO world heritage sites and natural landscapes

with more traditional impact metrics on population and economic assets illustrated that judgment on the severity of an event strongly depends on the exposure considered.

However, the risk modelling approach based on OSM exposure data has several limitations. The suitability of OSM for certain research purposes, as well as OSM data quality and data completeness have been discussed extensively (e.g., Zheng et al. 2021; Zhang et al. 2022). There is a large disparity in OSM coverage between countries and world regions, and between different types of assets (Herfort et al. 2023; Ludwig and Zipf 2019)

and attributes further describing these assets (Biljecki, Chow, and Lee 2023). Furthermore, as a crowd-sourced project, not all entries are checked for their accuracy (Zhou, Wang, and Liu 2022; Xie et al. 2019). Even for Switzerland, the extracted features are therefore by no means complete. While the rail network on OSM is mostly congruent with the official geospatial records¶ publicly provided by the Swiss government, only 11 of the 13 UNESCO World Heritage Sites in Switzerland were listed, and of the 58 prehistoric pile dwellings around the Alps, only five were included.

There are no future projections or reliable tracking of past exposure changes within OSM, which is predominantly a snap-shot of a moment in time. Thus, an assessment of past events or future risks can only be made with respect to current exposure or requires additional modeling techniques beyond the OSM realm[+]. Hence, the quality of the risk analysis based on OSM exposure data can vary significantly. Nevertheless, it is often the only freely available resource, and its catalog is continuously growing and improving.

On the technical side, the disaggregation step from OSM polygons and lines to CLIMADA point exposures, as well as the reaggregation of the impact values to these original polygon and line shapes, introduces imprecision owing to the finite resolution of the interpolation algorithm. The uncertainty related to the resolution can be assessed using Monte Carlo approaches (Kropf et al. 2022). The relative importance of this uncertainty with respect to all other risk model uncertainties from unknowns in the hazard, exposure, and vulnerability model must in general be assessed case by case and can be quantified with sensitivity analysis. Note that it is not possible to make a generic statement on the effect of resolution uncertainty on the risk model, as this depends strongly on the purpose of the study, the chosen output metrics, and the chosen set of modeled input uncertainties (Meiler et al. 2023).

Extracting features from OSM beyond the pre-written exposure category wrappers in the OSM-flex module can be cumbersome, as the required keys and values need to be identified, and often requires some back-and-forth iterative consultation of the OSM wiki [*] or OSM taginfo databases [♯]. The extracted features may further need to be post-processed to eliminate duplicates or simplify complex shapes. This may limit their wide use to non-expert practitioners in the field of climate risk modelling. However, these difficulties are inherent also to the few other open-source and well-maintained OSM feature extraction packages, of which we presented advantages and drawbacks for the use of natural hazard risk assessments. We showed that OSM-flex particularly excels for the use case of repeated, large-scale and highly customized spatial feature extraction within complex software environments where efficient dependency management is key.

Several other works seamlessly integrate OSM data for natural hazard risk calculations. For example, Koks, Rozenberg, et al. (2019) combined state-of-the-art global hazard map-

ping of cyclones, floods and earthquakes with approximately 50 mil. kilometer of transport network data included in OSM to study multi-hazard infrastructure risk and the viability of protection measures. And Nirandjan et al. (2022) extracted, categorized, and rasterized the world's main critical infrastructure systems into a global database, from which the Critical Infrastructure Spatial Index (CISI) is developed, which expresses the global spatial intensity of critical infrastructure and is used in several natural hazard risk studies ((e.g., Gnyawali et al. 2023) for landslides). Both studies draw on the extraction and processing source code for OSM data presented in section 2.1, which is now packaged into the OSM-flex module, and available to an even wider research audience.

More generally, this may open up complementary possibilities for areas of study that traditionally rely on other types of data sources such as satellite imagery (Stritih et al. 2021). In recent years, there has been a trend towards more holistic, quantitative views of the consequences of extreme weather events as opposed to focusing on monetary asset losses alone. Exemplary studies investigate, e.g., displaced population (Kam et al. 2021) or basic service disruptions (Mühlhofer, Koks, Kropf, et al. 2023). Wider quantitative perspectives will allow decision-makers to not inherently prioritize monetary elements because of the absence of other quantifiable criteria. Thus, the diverse indicators of natural hazard risk, towards which the here-presented approach contributes, can form the basis of multi-criteria adaptation decision frameworks (Velimirović, Janjić, and Velimirović 2023; Haque 2016; DiStefano and Krubiner 2020; Bowen 2002), leveling the playground with economic interests and allowing us to tackle questions such as the role of social inequalities, urban-land divides, and environmental justice (Gerber et al. 2012) in a (semi-)quantitative way.

## 5. Conclusion

OSM is a potent data source for informing multi-faceted climate risk analysis, and can support decision making with respect to climate adaptation, going beyond the common focus on (coarse-resolution) monetary asset values and population counts. Despite the limitations inherent to crowd-sourced open data, OSM can be used to freely retrieve a large variety of exposures with world-wide coverage. In this manuscript, we showcase risk assessment on healthcare facilities, railways, UN-ESCO World Heritage Sites, forests, and airports, but OSM can be used to retrieve an even larger variety of features: A non-exhaustive listing includes urban assets at single building scale; different land uses such as agriculture, forestry, or pastures; assets for different economic sectors such as mining, industrial manufacturing, commerce, energy or tourism; culturally relevant sites and regions; road networks; critical infrastructures for, e.g., education, water management, communication, energy supply; and ecological regions important for ecosystem service provision, biodiversity preservation, and leisure. We present OSM-flexas light-weight Python-based OSM extraction tool for any of these features. The seamless integration of OSM-flexinto the established open-source risk modelling framework CLIMADA promises that the methodology is applicable in academia, public institutions, the private sector, and the humanitarian sector.

## Acknowledgement

## Data Availability

All the data and source code are publicly available as mentioned in the manuscript. Scripts to reproduce results and result figures can be found at `https://github.com/Evelyn-M/osm-climate-risks`.

## References

Aznar-Siguan, Gabriela and David N. Bresch. "CLIMADA v1: A Global Weather and Climate Risk Assessment Platform". In: *Geoscientific Model Development* 12.7 (July 19, 2019), pp. 3085–3097. ISSN: 1991-959X. DOI: `10.5194/gmd-12-3085-2019`. (Visited on 05/11/2020).

Biljecki, Filip, Yoong Shin Chow, and Kay Lee. "Quality of Crowdsourced Geospatial Building Information: A Global Assessment of OpenStreetMap Attributes". In: *Building and Environment* 237 (June 1, 2023), p. 110295. ISSN: 0360-1323. DOI: `10.1016/j.buildenv.2023.110295`. (Visited on 05/04/2023).

Blass, Robert et al. *Automatic Generation of Winter Storm Warnings*. Technical Report 282. MeteoSwiss, 2022. URL: `https://doi.org/10.18751/pmch/tr/282.winterstormwarnings/1.0`.

Bloemendaal, Nadia, Ivan D. Haigh, et al. "Generation of a Global Synthetic Tropical Cyclone Hazard Dataset Using STORM". In: *Scientific Data* 7.1 (1 Feb. 6, 2020), p. 40. ISSN: 2052-4463. DOI: `10.1038/s41597-020-0381-2`. (Visited on 12/06/2021).

Bloemendaal, Nadia and Elco Koks. "Current and Future Tropical Cyclone Wind Risk in the Small Island Developing States". In: *Hurricane Risk in a Changing Climate*. Ed. by Jennifer M. Collins and James M. Done. Hurricane Risk. Cham: Springer International Publishing, 2022, pp. 121–142. ISBN: 978-3-031-08568-0. DOI: `10.1007/978-3-031-08568-0_6`. (Visited on 03/20/2023).

Boeing, Geoff. "OSMnx: New Methods for Acquiring, Constructing, Analyzing, and Visualizing Complex Street Networks". In: *Computers, Environment and Urban Systems* 65 (Sept. 1, 2017), pp. 126–139. ISSN: 0198-9715. DOI: `10.1016/j.compenvurbsys.2017.05.004`. (Visited on 03/20/2023).

Bossche, Joris Van den et al. *geopandas/geopandas: v0.13.2*. Version v0.13.2. June 2023. DOI: `10.5281/zenodo.8009629`. URL: `https://doi.org/10.5281/zenodo.8009629`.

Bowen, William M. *Environmental Justice Through Research-Based Decision-Making*. Routledge, May 3, 2002. 292 pp. ISBN: 978-1-135-57815-2. Google Books: `C_uOAgAAQBAJ`.

Bresch, David N. and Gabriela Aznar-Siguan. "CLIMADA v1.4.1: Towards a Globally Consistent Adaptation Options Appraisal Tool". In: *Geoscientific Model Development* 14.1 (Jan. 22, 2021), pp. 351–363. ISSN: 1991-959X. DOI: `10.5194/gmd-14-351-2021`. (Visited on 12/24/2021).

Bundesamt für Raumentwicklung ARE. *Flächennutzung*. URL: `https://www.are.admin.ch/are/de/home/raumentwicklung-und-raumplanung/grundlagen-und-`

daten / raumbeobachtung / siedlung / flaechennutzung . html (visited on 08/25/2023).

Center for International Earth Science Information Network (CIESIN), Columbia University. *Gridded Population of the World, Version 4 (GPWv4): Population Density, Revision 11*. Palisades, NY: Socioeconomic Data and Applications Center (SEDAC), 2017. DOI: 10 . 7927 / H49C6VHW. (Visited on 03/24/2023).

Cerri, Marco et al. "Are OpenStreetMap Building Data Useful for Flood Vulnerability Modelling?" In: *Natural Hazards and Earth System Sciences* 21.2 (Feb. 16, 2021), pp. 643–662. ISSN: 1561-8633. DOI: 10.5194/nhess - 21 - 643 - 2021. (Visited on 03/20/2023).

DiStefano, Michael J. and Carleigh B. Krubiner. "Beyond the Numbers: A Critique of Quantitative Multi-Criteria Decision Analysis". In: *International Journal of Technology Assessment in Health Care* 36.4 (Aug. 2020), pp. 292–296. ISSN: 0266-4623, 1471-6348. DOI: 10 . 1017 / S0266462320000410. (Visited on 03/21/2023).

Eberenz, Samuel et al. "Asset Exposure Data for Global Physical Risk Assessment". In: *Earth System Science Data* 12.2 (Apr. 9, 2020), pp. 817–833. ISSN: 1866-3508. DOI: 10.5194/essd-12-817-2020. (Visited on 05/14/2020).

Field, C.B et al. "IPCC, 2014: Summary for Policymakers." In: *Climate Change 2014: Impacts, Adaptation, and Vulnerability. Part A: Global and Sectoral Aspects. Contribution of Working Group II to the Fifth Assessment Report of the Intergovernmental Panel on Climate Change*. Cambridge: Cambridge University Press, 2014, p. 34.

Gaillard, Jean-Michel et al. "Effects of Hurricane Lothar on the Population Dynamics of European Roe Deer". In: *The Journal of Wildlife Management* 67.4 (2003), pp. 767–773. ISSN: 0022-541X. DOI: 10 . 2307 / 3802684. JSTOR: 3802684. (Visited on 03/21/2023).

GeoFabrik. *GEOFABRIK // Downloads*. URL: https : / / www . geofabrik . de / data / download.html (visited on 03/21/2023).

Gerber, Julien-François et al. *Guide to Multicriteria Evaluation for Environmental Justice Organisations*. 9. EJOLT, 2012.

Gnyawali, Kaushal et al. "Framework for Rainfall-Triggered Landslide-Prone Critical Infrastructure Zonation". In: *Science of The Total Environment* 872 (May 10, 2023), p. 162242. ISSN: 0048-9697. DOI: 10 . 1016 / j . scitotenv . 2023 . 162242. (Visited on 03/29/2023).

Gultom, Yohanes, Toto Haryanto, and Heru Suhartanto. "Route Subnetwork Generation Using OpenStreetMap Data for Emergency Response Problem Modeling in Indonesia". In: *2021 International Conference on Advanced Computer Science and Information Systems (ICACSIS)*. 2021 International Conference on Advanced Computer Science and Information Systems (ICACSIS). Oct. 2021, pp. 1–6. DOI: 10.1109/ICACSIS53237 . 2021.9631340.

Haque, Anika Nasra. "Application of Multi-Criteria Analysis on Climate Adaptation Assessment in the Context of Least Developed Countries". In: *Journal of Multi-Criteria Decision Analysis* 23.5-6 (2016), pp. 210–224. ISSN: 1099-1360. DOI: 10.1002/mcda.1571. (Visited on 03/21/2023).

Herfort, Benjamin et al. "A Spatio-Temporal Analysis Investigating Completeness and

Inequalities of Global Urban Building Data in OpenStreetMap". In: *Nat Commun* 14.1 (1 July 6, 2023), p. 3985. ISSN: 2041-1723. DOI: `10.1038/s41467-023-39698-6`. (Visited on 08/25/2023).

Hoffmann, Sarah and contributors. *PyOsmium.* Version 3.6.0. Jan. 21, 2023. URL: `https://osmcode.org/pyosmium/` (visited on 04/28/2023).

Jordahl, Kelsey et al. *Geopandas/Geopandas: V0.12.2.* Zenodo, Dec. 10, 2022. DOI: `10.5281/zenodo.7422493`. (Visited on 03/21/2023).

Jordi, Beat. *20 Jahre nach «Lothar»: Der Wald hat sein Terrain zurückerobert.* Apr. 12, 2019. URL: `https://www.bafu.admin.ch/bafu/de/home/themen/thema-wald-und-holz/wald-und-holz--dossiers/magazin2019-4-der-wald-hat-sein-terrain-zurueckerobert.html` (visited on 03/20/2023).

Kam, Pui Man et al. "Global Warming and Population Change Both Heighten Future Risk of Human Displacement Due to River Floods". In: *Environ. Res. Lett.* 16.4 (Mar. 2021), p. 044026. ISSN: 1748-9326. DOI: `10.1088/1748-9326/abd26c`. (Visited on 04/27/2021).

Koks, E. E., J. Rozenberg, et al. "A Global Multi-Hazard Risk Analysis of Road and Railway Infrastructure Assets". In: *Nature Communications* 10.1 (1 June 25, 2019), p. 2677. ISSN: 2041-1723. DOI: `10.1038/s41467-019-10442-3`. (Visited on 06/19/2020).

Koks, E.E. *DamageScanner: Python tool for natural hazard damage assessments.* 2022. DOI: `10.5281/zenodo.2551015`. URL: `http://doi.org/10.5281/zenodo.2551015`.

Koks, Elco Eduard, Ben Dickens, and Tom Russell. *Trade and tRAnsport Impact and fLow analysiS (TRAILS).* Zenodo, Oct. 21, 2022. DOI: `10.5281/zenodo.7234397`. (Visited on 03/21/2023).

Kropf, Chahan M. et al. "Uncertainty and Sensitivity Analysis for Probabilistic Weather and Climate-Risk Modelling: An Implementation in CLIMADA v.3.1.0". In: *Geoscientific Model Development* 15.18 (Sept. 23, 2022), pp. 7177–7201. ISSN: 1991-959X. DOI: `10.5194/gmd-15-7177-2022`. (Visited on 10/10/2022).

Ludwig, Christina and Alexander Zipf. "Exploring Regional Differences in the Representation of Urban Green Spaces in OpenStreetMap". In: *Geographical and Cultural Aspects of Geo-Information: Issues and Solutions.* AGILE 2019 Workshop. Cyprus, 2019.

Lüthi, Samuel et al. "Globally Consistent Assessment of Economic Impacts of Wildfires in CLIMADA v2.2". In: *Geoscientific Model Development* 14.11 (Nov. 25, 2021), pp. 7175–7187. ISSN: 1991-959X. DOI: `10.5194/gmd-14-7175-2021`. (Visited on 05/11/2022).

Meiler, Simona et al. *Unraveling Unknowns of Future Tropical Cyclone Risks.* Mar. 30, 2023. DOI: `10.21203/rs.3.rs-2703613/v1`. (Visited on 03/31/2023). preprint.

MeteoSwiss, Federal Office of Meteorology and Climatology. *Explanation of the danger levels - Wind.* URL: `https://www.meteoschweiz.admin.ch/wetter/gefahren/erlaeuterungen-der-gefahrenstufen/wind.html` (visited on 03/21/2023).

Microsoft. *GlobalMLBuildingFootprints.* Microsoft, Aug. 25, 2023. URL: `https://github.com/microsoft/GlobalMLBuildingFootprints` (visited on 08/25/2023).

Mühlhofer, Evelyn, Elco Koks, Lukas Riedel, et al. *Osm-Flex/Osm-Flex: V1.0.1.* Zenodo,

June 26, 2023. DOI: `10.5281/zenodo.8083066`. (Visited on 06/26/2023).

Mühlhofer, Evelyn, Elco E. Koks, Chahan M. Kropf, et al. "A Generalized Natural Hazard Risk Modelling Framework for Infrastructure Failure Cascades". In: *Reliability Engineering & System Safety* 234 (June 1, 2023), p. 109194. ISSN: 0951-8320. DOI: `10.1016/j.ress.2023.109194`. (Visited on 03/28/2023).

Mulholland, Eamonn and Luc Feyen. "Increased Risk of Extreme Heat to European Roads and Railways with Global Warming". In: *Climate Risk Management* 34 (Jan. 1, 2021), p. 100365. ISSN: 2212-0963. DOI: `10.1016/j.crm.2021.100365`. (Visited on 03/20/2023).

Niemeyer, Stefan and Peter Albisser. *Lothar: der Orkan 1999: Ereignisanalyse.* Birmensdorf: Eidg. Forschungsanstalt WSL, 2001. ISBN: 3-905620-93-6. URL: `https://www.wsl.ch/de/projekte/sturm-lothar.html` (visited on 03/21/2023).

Nirandjan, Sadhana et al. "A Spatially-Explicit Harmonized Global Dataset of Critical Infrastructure". In: *Sci Data* 9.1 (1 Apr. 1, 2022), p. 150. ISSN: 2052-4463. DOI: `10.1038/s41597-022-01218-4`. (Visited on 03/13/2023).

OpenStreetMap contributors. *OpenStreetMap Wiki.* URL: `https://wiki.openstreetmap.org/wiki/Main_Page` (visited on 08/25/2023).

— *Osmosis.* Version 0.48.3. URL: `https://wiki.openstreetmap.org/wiki/Osmosis` (visited on 04/28/2023).

Pagani, Marco et al. *The OpenQuake-engine User Manual. OpenQuake Manual for Engine Version 3.17.2.* Global Earthquake Model (GEM) Foundation, 2022. URL: `10.13117/GEM.OPENQUAKE.MAN.ENGINE.%203.17.2`.

Paulik, Ryan et al. "RiskScape: A Flexible Multi-Hazard Risk Modelling Engine". In: *Nat Hazards* (Sept. 17, 2022). ISSN: 1573-0840. DOI: `10.1007/s11069-022-05593-4`. (Visited on 08/25/2023).

Pörtner, H.-O. et al. *Climate Change 2022: Impacts, Adaptation and Vulnerability.* Technical Summary. Cambridge, UK and New York, USA: Cambridge University Press, 2022, pp. 37–118. ISBN: 978-1-00-932584-4.

Potapov, Peter et al. "The Global 2000-2020 Land Cover and Land Use Change Dataset Derived From the Landsat Archive: First Results". In: *Frontiers in Remote Sensing* 3 (2022). ISSN: 2673-6187. DOI: `10.3389/frsen.2022.856903`. URL: `https://www.frontiersin.org/articles/10.3389/frsen.2022.856903`.

Röösli, Thomas and David N. Bresch. *Probabilistic Windstorm Hazard Event Set for Europe.* ETH Zurich, Mar. 25, 2020. DOI: `10.3929/ethz-b-000406567`. (Visited on 05/22/2023).

Ruckelshaus, Mary et al. "Harnessing New Data Technologies for Nature-Based Solutions in Assessing and Managing Risk in Coastal Zones". In: *International Journal of Disaster Risk Reduction* 51 (Dec. 1, 2020), p. 101795. ISSN: 2212-4209. DOI: `10.1016/j.ijdrr.2020.101795`. (Visited on 03/20/2023).

Schmid, Emanuel. *CLIMADA Data API.* Version 2.0.0. 2023. URL: `https://climada.ethz.ch/data-api/v2/docs` (visited on 05/23/2023).

Schotten, Roman and Daniel Bachmann. "Critical Infrastructure Network Modelling for Flood Risk Analyses: Approach and Proof of Concept in Accra, Ghana". In: *Journal of Flood Risk Management* n/a.n/a (2023), e12913. ISSN: 1753-318X.

DOI: `10.1111/jfr3.12913`. (Visited on 05/22/2023).

Severino, Luca G. et al. "Projections and Uncertainties of Future Winter Windstorm Damage in Europe". In: *EGUsphere* (Feb. 14, 2023), pp. 1–31. DOI: `10.5194/egusphere-2023-205`. (Visited on 03/02/2023).

Stritih, Ana et al. "Addressing Disturbance Risk to Mountain Forest Ecosystem Services". In: *Journal of Environmental Management* 296 (Oct. 15, 2021), p. 113188. ISSN: 0301-4797. DOI: `10.1016/j.jenvman.2021.113188`. (Visited on 03/20/2023).

Tenkanen, Henrikki. *Pyrosm - OpenStreetMap PBF Data Parser for Python*. Version v0.5.1/2. May 11, 2020. URL: `https://pyrosm.readthedocs.io` (visited on 08/27/2020).

Topf, Jochen. *Osmcode/Osmium-Tool*. Version 1.15.0. Jan. 19, 2023. URL: `osmcode.org/osmium-tool/` (visited on 08/25/2023).

UNDRR. *Sendai Framework for Disaster Risk Reduction 2015-2030*. UNDRR, 2015. URL: `https://www.undrr.org/publication/sendai-framework-disaster-risk-reduction-2015-2030` (visited on 11/26/2021).

Van Ginkel, Kees C. H. et al. "Flood Risk Assessment of the European Road Network". In: *Natural Hazards and Earth System Sciences* 21.3 (Mar. 15, 2021), pp. 1011–1027. ISSN: 1561-8633. DOI: `10.5194/nhess-21-1011-2021`. (Visited on 03/20/2023).

Velimirović, Lazar Z., Aleksandar Janjić, and Jelena D. Velimirović. "Multi-Criteria Decision-Making Methods Based on Fuzzy Sets". In: *Multi-Criteria Decision Making for Smart Grid Design and Operation: A Society 5.0 Perspective*. Ed. by Lazar Z. Velimirović, Aleksandar Janjić, and Jelena D. Velimirović. Disruptive Technologies and Digital Transformations for Society 5.0. Singapore: Springer Nature, 2023, pp. 9–25. ISBN: 978-981-19767-7-3. DOI: `10.1007/978-981-19-7677-3_2`. (Visited on 03/21/2023).

Virot, E. et al. "Critical Wind Speed at Which Trees Break". In: *Phys. Rev. E* 93.2 (Feb. 2, 2016), p. 023001. DOI: `10.1103/PhysRevE.93.023001`. (Visited on 03/20/2023).

Weber, Markus. *Osmconvert*. Version 0.8.11. Nuernberg, Mar. 31, 2020. URL: `http://m.m.i24.cc/osmconvert.c` (visited on 04/28/2023).

Welker, Christoph, Thomas Röösli, and David N. Bresch. "Comparing an Insurer's Perspective on Building Damages with Modelled Damages from Pan-European Winter Windstorm Event Sets: A Case Study from Zurich, Switzerland". In: *Natural Hazards and Earth System Sciences Discussions* (Apr. 23, 2020), pp. 1–31. ISSN: 1561-8633. DOI: `10.5194/nhess-2020-115`. (Visited on 12/15/2020).

WorldPop and Center for International Earth Science Information Network (CIESIN), Columbia University. *Global High Resolution Population Denominators Project*. University of Southampton, 2020. DOI: `10.5258/SOTON/WP00660`. (Visited on 08/25/2023).

Xie, Xuejing et al. "OpenStreetMap Data Quality Assessment via Deep Learning and Remote Sensing Imagery". In: *IEEE Access* 7 (2019), pp. 176884–176895. ISSN: 2169-3536. DOI: `10.1109/ACCESS.2019.2957825`.

Yamazaki, Dai et al. "A Physically Based Description of Floodplain Inundation Dynamics in a Global River Routing Model".

In: *Water Resources Research* 47.4 (2011). ISSN: 1944-7973. DOI: 10 . 1029 / 2010WR009726. (Visited on 08/29/2023).

Yesudian, Aaron N. and Richard J. Dawson. "Global Analysis of Sea Level Rise Risk to Airports". In: *Climate Risk Management* 31 (Jan. 1, 2021), p. 100266. ISSN: 2212-0963. DOI: 10.1016/j.crm.2020.100266. (Visited on 03/20/2023).

Zhang, Yuheng et al. "Assessing OSM Building Completeness Using Population Data". In: *International Journal of Geographical Information Science* 36.7 (July 3, 2022), pp. 1443–1466. ISSN: 1365-8816. DOI: 10. 1080/13658816.2021.2023158. (Visited on 03/21/2023).

Zheng, Guoxiong et al. "Increasing Risk of Glacial Lake Outburst Floods from Future Third Pole Deglaciation". In: *Nat. Clim. Chang.* 11.5 (5 May 2021), pp. 411–417. ISSN: 1758-6798. DOI: 10.1038/s41558-021-01028-3. (Visited on 03/20/2023).

Zhou, Qi, Shuzhu Wang, and Yaoming Liu. "Exploring the Accuracy and Completeness Patterns of Global Land-Cover/Land-Use Data in OpenStreetMap". In: *Applied Geography* 145 (Aug. 1, 2022), p. 102742. ISSN: 0143-6228. DOI: 10.1016/ j . apgeog . 2022 . 102742. (Visited on 03/21/2023).

## Appendix A. OSM-flex module

The main steps in the OSM feature extraction process using the OSM-flex package, introduced in section 2.1, are explained in more detail in the following paragraphs. The OSM-flex package is available on GitHub (`https://github.com/osm-flex/osm-flex`) and as PyPI package (Mühlhofer, Koks, Riedel, et al. 2023). The modules available within the OSM-flex package are structured according to the previously introduced fours steps.

*Appendix A.1. Download*

OSM data is downloaded in Protocolbuffer Binary Format (PBF; see `https://wiki.openstreetmap.org/wiki/PBF_Format` for further description). Automated download options are currently available for the entire planet file (retrieved from `https://planet.openstreetmap.org/pbf/planet-latest.osm.pbf`), for world regions (Africa, Antarctica, Asia, Australia and Oceania, Central America, Europe, North America, South America) and for all countries available on, for example, `download.geofabrik.de`. If the desired region or country is not available via the download-API, it is recommended to clip the desired area from a larger source file (see next step).

As OSM is a crowd-sourced and living project, mapped data constantly evolves. To prevent data sources from becoming outdated when working on them for a longer time span, it is recommended to update the source files occasionally. Two options are conceivable: re-downloading the entire data dump of concern (allowing for existing files to be overwritten in the respective command) or updating the already downloaded files on a recurring basis, using diffs (*.osc.gz). Such diffs are provided at various timestamps from different extract providers, for instance daily via `download.geofabrik.de` or minutely via `download.openstreetmap.fr`.

*Appendix A.2. Clip*

This optional step of clipping (cutting) larger source files to any user-defined area requires a one time installation of either osmconvert ((Weber 2020)) or osmosis ((OpenStreetMap contributors 2023b). More command line executables for handling *.osm.pbf files exist, some of which are available via pip and conda distribution channels, such as pyOsmium ((Topf 2023; Hoffmann and contributors 2023)). However, not all of those currently support all operating systems, which is why the OSM-flex package gives preference to osmconvert and osmosis.

There are three ways to specify the area to which to clip: by passing a bounding box (the corners of a geographical rectangle), passing a shapely (multi-)polygon, or passing a Polygon filter file (*.poly; see `https://wiki.openstreetmap.org/wiki/Osmosis/Polygon_Filter_File_Format` for further description) containing the (multi-)polygon outline information.

Convenience functions are available to obtain country and admin-1 shapes within the OSM-flex package, and there are several ways to obtain .poly files externally (for example, `https://github.com/jameschevalier/cities` for a good description of how to find and obtain them via `http://polygons.openstreetmap.fr/`, and for a .poly file collection of many cities of the world). It should be noted that clipping to (multi-)polygons requires the creation of a

temporary .poly file under the hood, and that OSM-flex provides a simplification method for complex shapes owing to file size restrictions. Clipping may take a while, and this process is faster if the source file is smaller (e.g. when taking a region file instead of the entire planet file to clip a contained sub-region).

*Appendix A.3. Extract*

There are two broad ways to extract OSM features into tabular (Geo)Pandas (Jordahl et al. 2022) format: via predefined wrappers for some frequently-used exposure categories, or via defining user-specific queries. Extraction wrappers are currently available for assets of many critical infrastructure sectors such as road, rail and air transportation, power, telecommunication, gas, healthcare and education. For user-defined queries, keys, key-value pairs or logic concatenations of these are allowed, together with a specification of which additional attribute keys should be parsed as columns the output table, and which geometry types should be considered. Finding suitable OSM keys or key-value pairs can be challenging at first, yet useful information may be obtained via the OSM wiki map feature documentation (`https://wiki.openstreetmap.org/wiki/Map_features`) or the OSM tag-info webpage (`https://taginfo.openstreetmap.org/`). There are some particularities when extracting uncommon features with may not yet be "registered" in the osmconf.ini file, which comes with the distribution. In such cases, the unknown keys must be manually added in the corresponding sections of the file.

*Appendix A.4. Post-process*

The following is a non-exhaustive list of common post-processing tasks which may be needed. Some are already part of this package, with more methods in development:

- simplifying networked geo-data (e.g. roads, rails, power lines): see for instance the "trails" package (Koks, Dickens, and Russell 2022)
- removing duplicates (same amenities with slightly different names) and near-duplicates (e.g., amenities may be marked as points, but building-shapes of the same amenities are also collected as multi-polygons): for example GeoPandas sjoin with a certain buffer tolerance (e.g. 100m, ..)
- removing small multi-polygon shapes in large multi-polygon based results (e.g. forest outlines) by filtering polygon area (a built-in shapely geometry attribute)

## Appendix B. Comparison of OSM-flex with other OSM-based tools

A plethora of helper tools exist to handle OSM data. Low-level command line tools such as osmosis (OpenStreetMap contributors 2023a), (Py)Osmium (Hoffmann and contributors 2023; Topf 2023), and osmconvert (Weber 2020) have basic functionalities for getting information about an OSM file, converting OSM file formats (such as .xml, .pbf, and .o5m), merging change files (diffs) or clipping geographical areas from an OSM file to a new OSM file.

On the side of maintained, well-documented and user-friendly Python-based parsing tools for OSM features, OSMnx and Pyrosm are two frequently used packages. Table B1 presents a brief comparison between these and OSM-flex, to guide potential users in selecting the adequate tool.

**Table B1.** Comparison of OSM-flexV1.0.1 with commonly used Python-based OSM parsing tools Pyrosm V0.6.1 and OSMnx V1.6.0

|  | OSM-flex | Pyrosm | OSMnx |
|---|---|---|---|
| Source of OSM data | .osm.pbf data dumps | .osm.pbf data dumps | overpass API |
| Continuous integration & testing | yes | yes | yes |
| Documentation | yes | yes | yes |
| Active development | yes | no[a] | yes |
| License | GPL-3.0 | MIT | MIT |
| Distribution channels | GitHub, pip | GitHub, pip[b], conda | GitHub, pip[b], conda |
| Package dependencies | Geopandas, cartopy | Geopandas, Pygeos, Cython, Pyrobuf and Cykhash, OSMnx | Geopandas, igraph, networkX, and many others |
| Feature cleaning & simplification | yes[c] | no | yes |
| Graph analysis | no | no[d] | yes |
| Parsing from bounding boxes | yes[e] | yes[f] | yes |
| Parsing from polygons | yes[e] | no | yes |
| Parsing from address | no | no | yes |
| Suitable for large queries | yes | yes | no |
| Suitable for queries on any user-defined tags | yes | yes | yes |
| Availability of pre-written common queries | yes (many infrastructure sectors) | yes (streets, buildings, POIs, landuse) | yes (buildings, many road classes) |
| Integration in risk model | yes[g] | no | no |

[a] no code development within past 365 days; [b] limited guarantee of success due to complex package dependencies; [c] simple filtering and duplicate removal, [d] util functions for export to igraph or networkX graphs via OSMnx available; [e] python-based wrappers requiring pre-installation of osmosis or osmconvert; [f] inefficient for very large data sets; [g] seamless integration with CLIMADA (Aznar-Siguan and Bresch 2019) and DamageScanner (Koks 2022).

OSM-flex is closer in its implementation logic to Pyrosm. Two main advantages are the lower dependency requirements and the possibility to clip arbitrary user-defined geographical shapes from the data dumps (i.e. pre-perform a geographical filtering). Due to its implementation in Cython, Pyrosm might on the other hand be slightly faster in parsing data where no geographical

filtering is applied. If only few OSM features are queried, or (road) network analysis should be performed, OSMnx is likely the best tool at hand.

## Appendix C. Lines and Polygons utility module

This utility module disaggregates line and polygon geometries into points, which, for instance, is necessary to spatially overlay (or, essentially, point-match) hazard footprints and exposures in CLIMADA impact calculations.

The desired disaggregation resolution can be specified in units of either the original coordinate reference system (crs) or in metres. In the latter case, geometries are automatically re-projected to a metre-based cylindrical projection centered around the object's central coordinate, to minimize distortions from the re-projection. For polygons, a regular raster of the chosen resolution is created and all points of the raster inside of a polygon are assigned to it. For polygons smaller than the raster resolution, at least one single point inside the polygon is assigned (even if this point is not part of the raster). Note that one does thus not have a common raster for all polygons, but one raster per object (since each object uses its own centered projection). Users that want to use a common raster can define one for the disaggregation (the re-projection must then be performed by the user). Lines are divided into segments equal in length in such a way that the total length of all lines is preserved. This is achieved by first computing the number of points $N$ per line by dividing the line length by the resolution and rounding the result. The minimum number of points is one. Second, the line is divided into corresponding $N + 1$ equal-length segments, and the points are placed in the middle of the segments.

More precisely, the number of points a line is divided in is

$$N = \max\left[\text{round}[(l/r) - 1)], 1\right] \tag{C.1}$$

with $l$ the total length of the line and $r$ the resolution. The effective resolution of the line is then

$$r_e = \frac{L}{N}. \tag{C.2}$$

These $N$ points are then distributed on the line at fractions of the line lengths starting from $r_e/2$

$$f_1 = r_e/2 \; ; \; f_2 = r_e \; ; \; f_3 = 3r_e/2 \; , \; \ldots. \tag{C.3}$$

Several examples are listed in Table C1.

The exposure value associated with each original line or polygon geometry can then either be divided equally among all points or be assigned wholly to each point. The former is typically used to disaggregate quantitative values such as the number of people, or to compute relative affected areas by disaggregating the value 1 over each geometry. The latter can be used to assign the area of the corresponding raster cell to each raster point, or the length of the corresponding line element to each line point, or to propagate qualitative values such as an ecosystem type. Note that the disaggregation leads to a certain distortion of the values, in particular, due to

**Table C1.** Disaggregation examples for lines of varying lengths and target resolutions.

| Length | Resolution | Number Points | Effective resolution | Fractions |
|--------|-----------|---------------|---------------------|-----------|
| l=1 | r=2 | N=1 | $r_e = 1$ | $f_1 = 0.5$ |
| l=1 | r=0.8 | N=1 | $r_e = 1$ | $f_1 = 0.5$ |
| l=1 | r=0.6 | N=2 | $r_2 = 0.5$ | $f_1 = 0.25, f_2 = 0.75$ |
| l=1 | r=0.4 | N=2 | $r_e = 0.25$ | $f_1 = 0.25, f_2 = 0.75$ |
| l=1 | r=0.2 | N=5 | $r_e = 0.2$ | $f_1=0.1, \quad f_2=0.3, \quad f_3=0.5, f_4=0.7, f_5=0.9$ |

boundary effects, and the user should carefully choose the resolution of the raster to fit the purpose of the study. One way to check the approximation resulting from the disaggregation step is to re-aggregate the values by geometry and compare.

## Appendix D. Application: Input data and method details

*Appendix D.1. OpenStreetMap queries*

The exposures used for the impact computation reported in Table 1 and 2 were based on the GeoDataFrames retrieved with the OSM-flexmodule using the OSM tags (keys and values) as described in Table D1. Note that for the critical infrastructures 'Healthcare facilities' and 'Airports', a single-line helper function is implemented within the CLIMADA OpenStreetMap module, which facilitates common queries.

**Table D1.** OSM tags (keys and values) and geometry types, which were extracted from the osm.pbf data dump for the respective exposure types, using the OSM-flexpackage

| Exposure Type | OSM Keys | OSM Values | Geometry Type |
|---------------|----------|-----------|---------------|
| Healthcare facilities | 'amenity' 'building' 'healthcare' | 'hospital' or 'doctors' 'hospital' or 'clinic' 'hospital' or 'clinic' or 'doctors' | points, multipolygons |
| Railways | 'railway' | 'rail' or 'tram' or 'light_rail' or 'narrow_gauge' | lines |
| Airports | 'aeroway' | 'aerodrome' | multipolygons |
| UNESCO sites | 'heritage_operator' | 'whc' | points, multipolygons |
| Forests | 'landuse' | 'forest' | multipolygons |

*Appendix D.2. Hazard, Exposure, and Vulnerability Data*

Fig. D1 displays the winter storm hazard footprints retrieved from the CLIMADA data API (Schmid 2023). Fig. D2 displays exposures for Switzerland, retrieved using the OSM-flex module, and fig. D3 asset value distributions from LitPop (Eberenz et al. 2020) and gridded population density (Center for International Earth Science Information Network (CIESIN), Columbia University 2017). Fig D4 displays impact functions (vulnerability curves) wind storm intensity to expected exposure impacts.
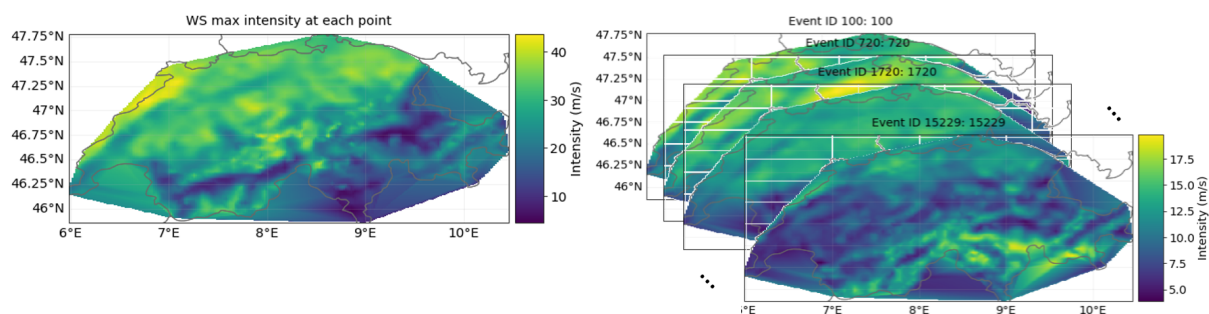


**Figure D1.** Winter storm hazard footprints (maximum 1-minutes sustained wind speed over 3-days) of Lothar (left) and of the WISC probabilistic extension hazard set for current climate (right) from (Röösli and Bresch 2020; Welker, Röösli, and Bresch 2020).
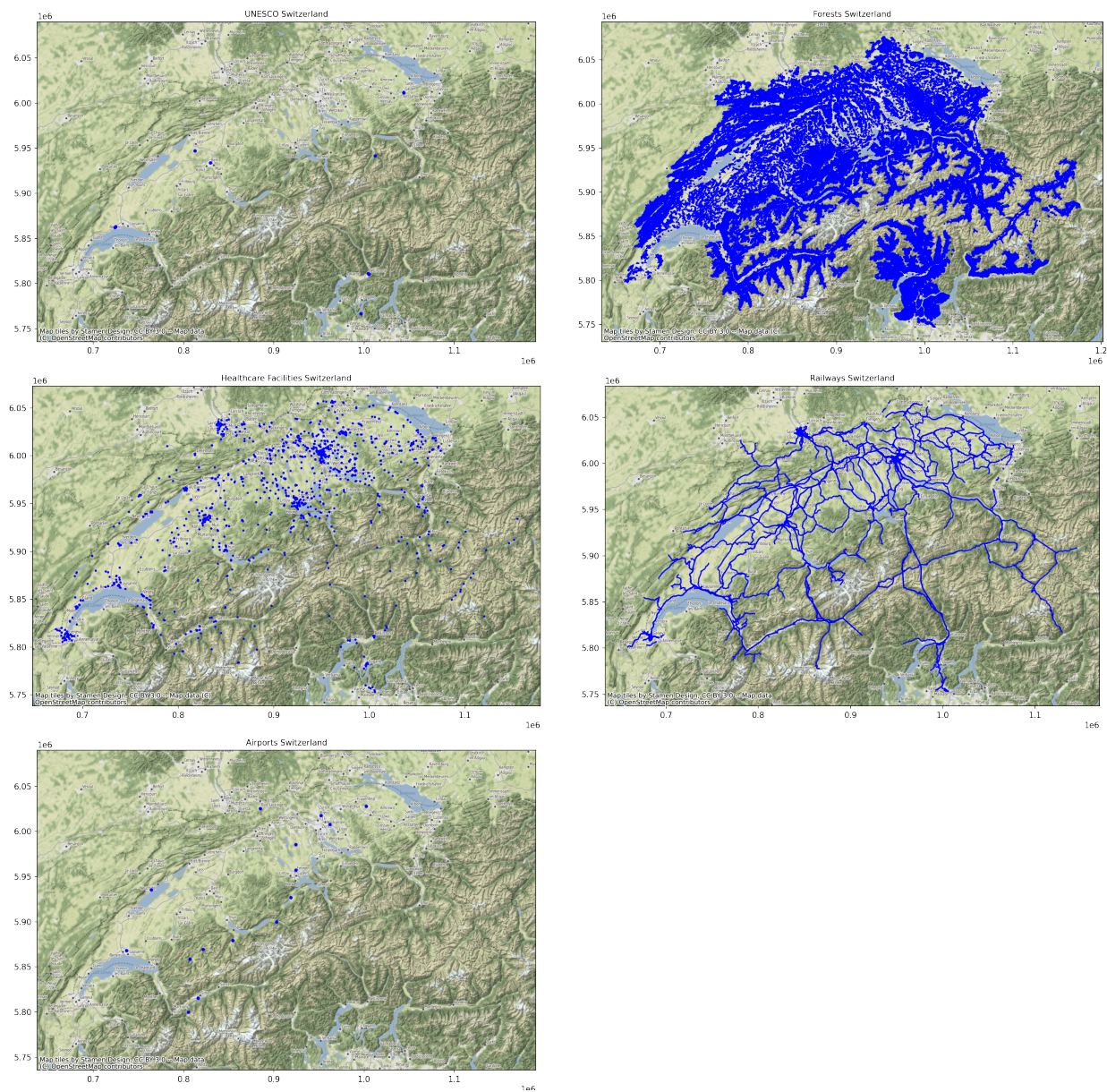
**Figure D2.** Exposure data extracted with the OSM-flexmodule (UNESCO heritage sites, forests, healthcare facilities, railways, airports) after post-processing (removal of duplicates, removal of polygons with area below $1\,000$ m$^2$)
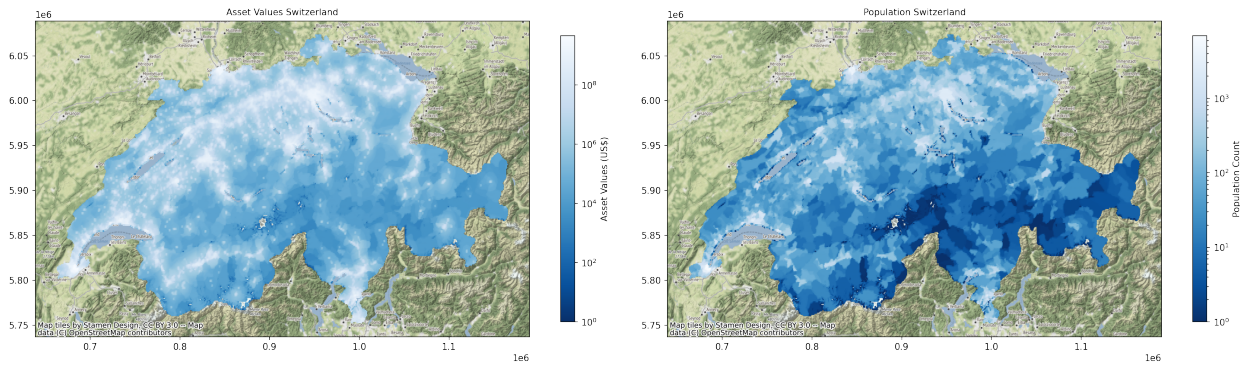
**Figure D3.** Exposure data often used for climate risk assessment: asset value distributions from LitPop (Eberenz et al. 2020), and gridded population density (Center for International Earth Science Information Network (CIESIN), Columbia University 2017).
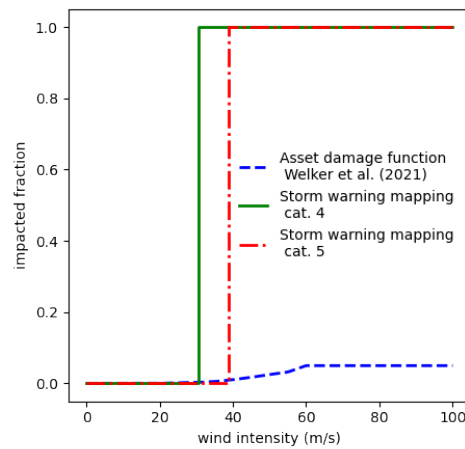


**Figure D4.** Impact functions employed for event impact and risk computations from winter storms for asset damages (blue, based on (Welker, Röösli, and Bresch 2020)), for affected healthcare facilities, UNESCO heritage sites, population and railways (green, based on the Federal Office for Meteorology and Climatology's warning category 4 wind-speed threshold (110 km/h or 30.5 m/s), and for forest loss (red, based on the warning category 5 wind-speed threshold (140 km/h or 38.9 m/s)).
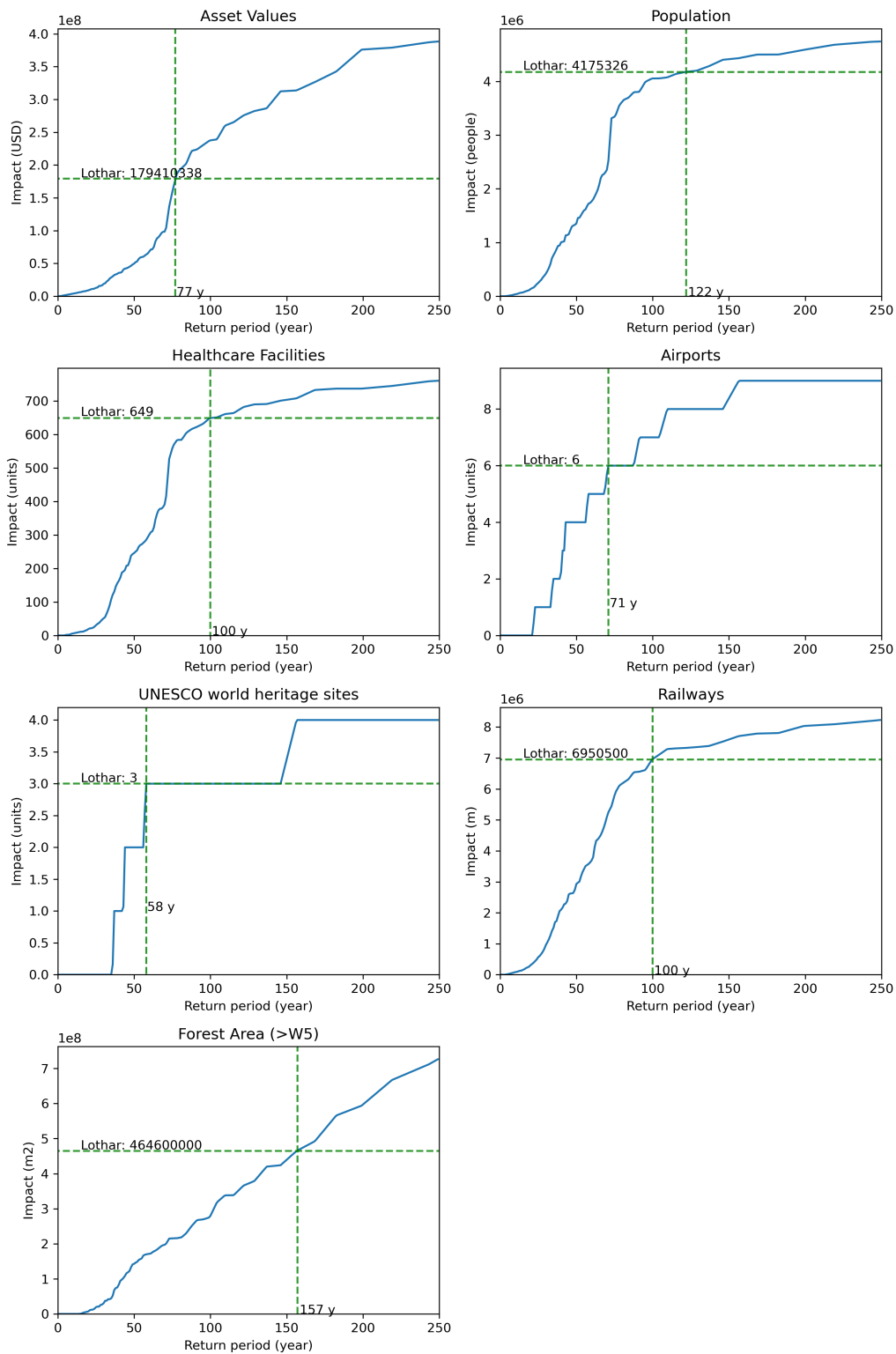
**Figure D5.** Return period curves of winter storm impacts for all exposure data categories used in this work's climate risk assessment, computed from the WISC probabilistic extension hazard set for current climate from (Röösli and Bresch 2020; Welker, Röösli, and Bresch 2020). Historic impacts from winter storm Lothar are indicated on the vertical axis, the corresponding computed return period values of these impacts are indicated on the horizontal axis.
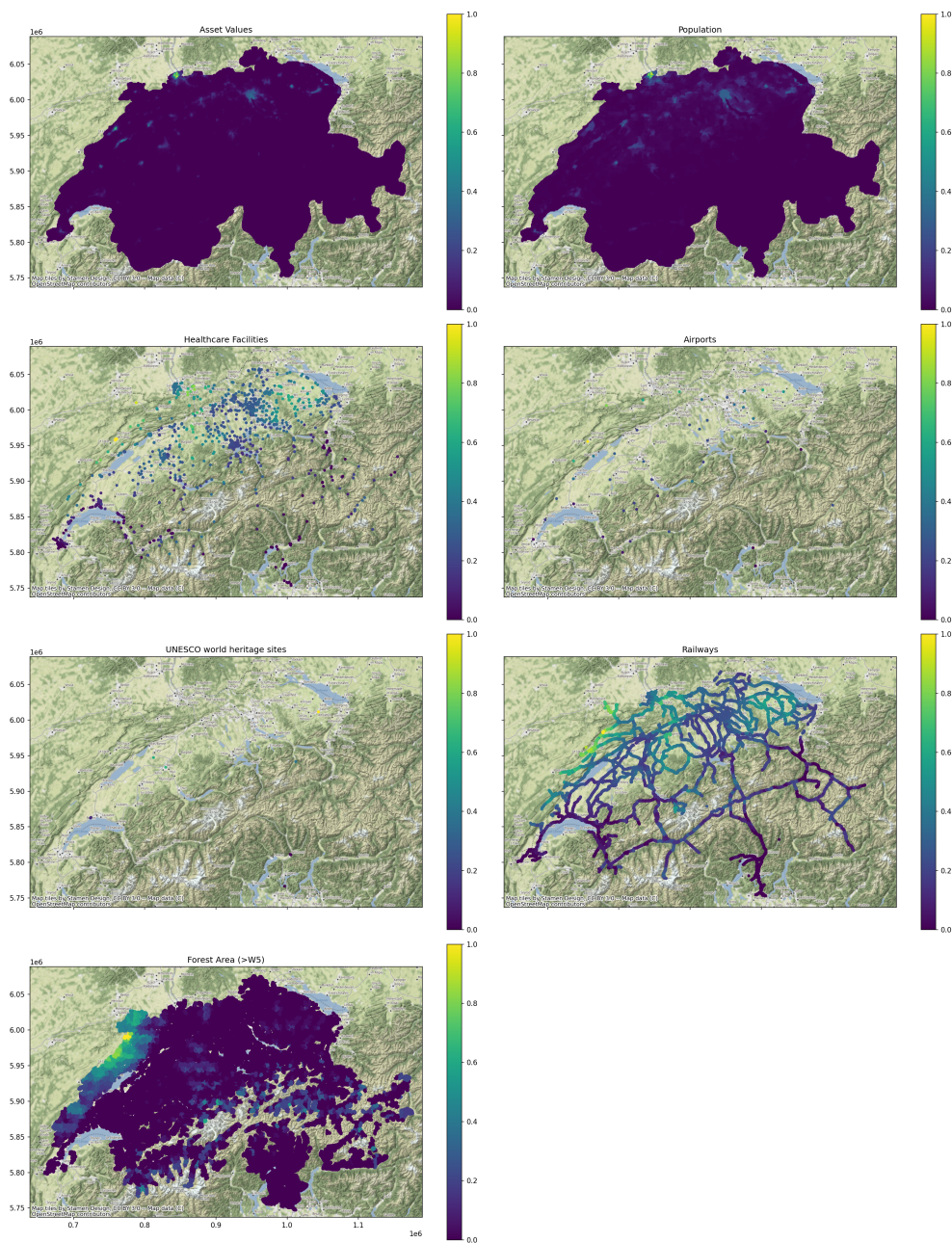
**Figure D6.** Normalized average expected annual impact derived from the probabilistic winter storm set (c.f. Fig.D1) for all exposures (c.f. Figs. D2, D3). For each exposure type individually, the impacts are normalized by the maximum impact over all points. The relative value highlights the impact hotspots for all exposure types.